

APPLICATION OF A  ${}^6\text{LiD}$  THERMAL-14 MeV NEUTRON CONVERTER  
TO THE MEASUREMENT OF ACTIVATION CROSS SECTIONSKatsuhei Kobayashi and Itsuro Kimura\*  
Research Reactor Institute, Kyoto University  
Kumatori-cho, Sennan-gun, Osaka 590-04 Japan

**Abstract:** By means of the following two reactions;  ${}^6\text{Li} + n_{\text{th}} \rightarrow {}^4\text{He} + \text{T} + 4.8 \text{ MeV}$  and  $\text{D} + \text{T} \rightarrow {}^4\text{He} + n$ , 14 MeV neutrons can be generated from thermal neutrons, whose flux conversion rate is estimated about  $2 \times 10^{-4}$ . A  ${}^6\text{LiD}$  converter, 10 x 10 cm square and 1 cm thick was prepared, and installed in a large thermal neutron irradiation facility of the Kyoto University Reactor, KUR, where the 14 MeV neutron flux of about  $2.5 \times 10^5 \text{ n/cm}^2/\text{sec}$  was obtained.

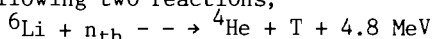
The characteristics of the  ${}^6\text{LiD}$  converters were measured: (1) energy of neutrons produced was determined to be  $14.05 \pm 0.07 \text{ MeV}$  by the reaction rate ratio of  ${}^{90}\text{Zr}(n,2n)/{}^{93}\text{Nb}(n,2n)$ , and (2) the energy spectrum was obtained by unfolding multi-foil activation data using the NEUPAC code.

Making use of the 14.1 MeV neutrons, twenty three kinds of activation cross sections were measured relative to that for the  ${}^{27}\text{Al}(n,\alpha){}^{24}\text{Na}$  reaction as a standard value. The present results have been compared with the evaluated data in ENDF/B-V and JENDL-2 and with the data in the IAEA Handbook and with the recent measurement by Ikeda et al.

( ${}^6\text{LiD}$ , D-T reaction, neutron converter, 14 MeV neutrons, Zr/Nb reaction ratio, spectrum unfolding, multi-foil, activation cross sections)

INTRODUCTION

The deuterium-tritium (D-T) reaction is a well known fusion reaction which produces 14 MeV neutrons. This process is usually performed by accelerator devices to generate the fast neutrons. On the other hand, there are several reports which have tried to get an alternative source of 14 MeV neutrons/1-3/. Lithium-6 interacts with thermal neutrons and create energetic tritons which can subsequently interact with deuterium to convert thermal neutrons to 14 MeV neutrons through the following two reactions;



The flux conversion rate of thermal neutrons to 14 MeV neutrons is about  $2 \times 10^{-4}/1-3/$ .

In the present work,  ${}^6\text{LiD}$  samples have been packed into an aluminum case and prepared as a thermal-14 MeV neutron converter, and the characteristics for the neutron energy and spectrum have been measured. Neutron energy from the D-T source is often determined by the kinematic relation of the  $\text{T}(d,n){}^4\text{He}$  reaction depending on the accelerating energy of deuteron and the emission angle of neutrons. As one of the practical techniques to measure the neutron source energy, an activation method has been proposed to take the reaction rate ratio between the  ${}^{90}\text{Zr}(n,2n)$  and  ${}^{93}\text{Nb}(n,2n)$  reactions/4/. The ratio method has been applied to the present measurement of neutron energy from the  ${}^6\text{LiD}$  converters. Activation data

have also been used to obtain the energy spectrum of neutrons from the converters. The NEUPAC code/5,6/ was employed to unfold the multi-foil activation data and the result was compared with that calculated by a one dimensional transport code, ANISN/7/. After the characteristics of the  ${}^6\text{LiD}$  converters were obtained, the fast neutrons of 14 MeV were applied to the measurement of twenty three kinds of activation cross sections by using the reference monitor for the  ${}^{27}\text{Al}(n,\alpha)$  reaction as a standard.

EXPERIMENTAL METHOD ${}^6\text{LiD}$  Converters

For the preparation of a  ${}^6\text{LiD}$  converter, a mass of the  ${}^6\text{LiD}$  sample was broken into pieces, and about 75 grams of the  ${}^6\text{LiD}$  sample was packed in an aluminum case of 10 x 10 cm square and 1 cm thick. The case was sealed up by the epoxy resin. The enrichment of  ${}^6\text{Li}$  is 95.5 %. Activation foils were sandwiched by a pair of the  ${}^6\text{LiD}$  converters.

Experimental Arrangement

Activation foils were 12.7 mm in diameter and 0.1 to 0.5 mm in thickness. The purity in each foil was more than 99 %. The sample foils, including aluminum foils for the reference cross section, were put between the pair of  ${}^6\text{LiD}$  converters, and these samples were set near the center of the aluminum case within the radius of about 1.5 cm. The converters and the sample foils were installed in the heavy water facility/8/ of the Kyoto University Reactor, KUR. The experimental arrangement is illustrated in Fig. 1. The irradiation room is about 2.4 x 2.4 x 2.4 cubic m. The converters were put away 20 cm from

\* Present address: Department of Nuclear Engineering, Faculty of Nuclear Engineering, Kyoto University, Yoshida-honmachi, Sakyo-ku, Kyoto 606

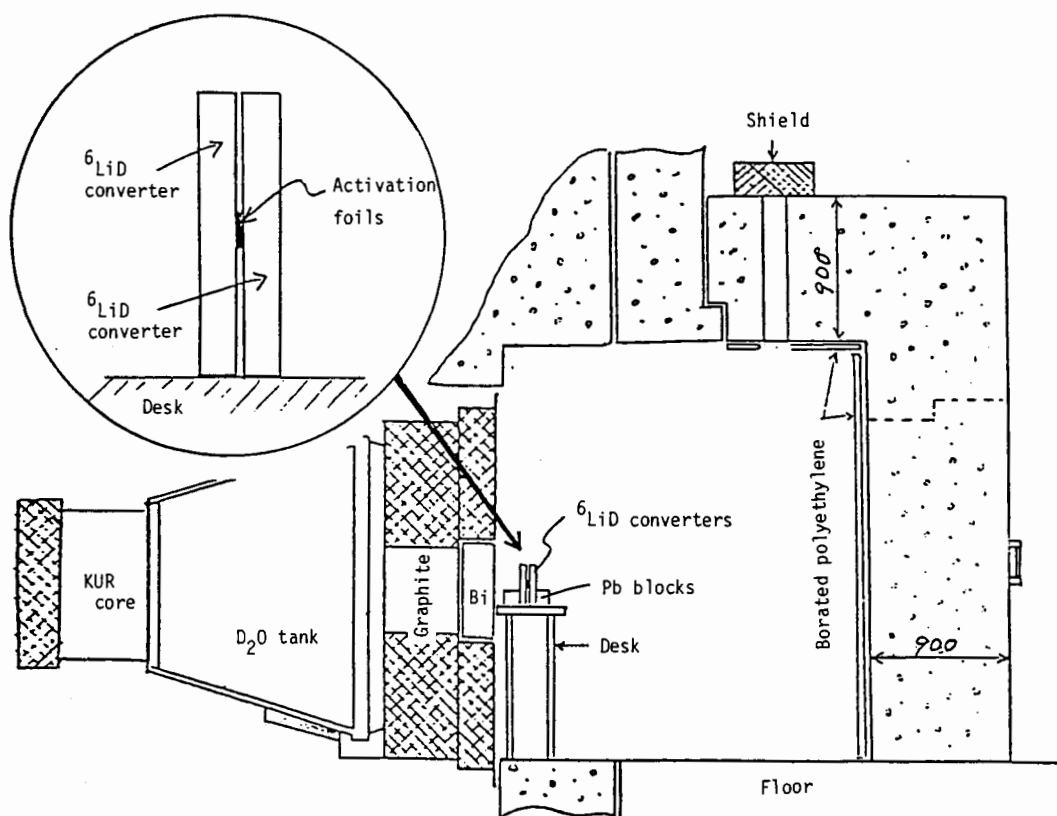


Fig. 1 Experimental arrangement for the measurement using  ${}^6\text{LiD}$  converters

the bismuth surface. Since the thermal neutron flux of about  $1.5 \times 10^9$  n/cm<sup>2</sup>/sec was obtained on the front surface of the converters during the 5 MW operation of KUR, the fast neutron flux of about  $2.5 \times 10^5$  n/cm<sup>2</sup>/sec was measured with the aluminum foil for the  ${}^{27}\text{Al}(n,\alpha)$  reaction. Then, the conversion rate presently obtained from thermal neutrons to 14.1 MeV neutrons has been observed to be close to that reported before/1-3/.

#### Inradiation and Activity Measurement

Two kinds of activation measurements have been performed; one is that for the measurement of neutron energy and spectrum from the  ${}^6\text{LiD}$  converters and the other is for the application to the measurement of activation cross sections. For the energy determination, Zr and Nb foils have been irradiated together and the reaction rate ratio for the (n,2n) reactions have been measured. To obtain the energy spectrum of neutrons from the converters, thirteen kinds of activation data have been unfolded by the NEUPAC code. In the measurement of activation cross sections with the converters, several sets of irradiations have been performed for about 70 hours in each run, and twenty three kinds of reaction cross sections have systematically been measured relative to that for the  ${}^{27}\text{Al}(n,\alpha)$  reaction, as a standard value.

After the irradiation, gamma-rays from the induced activities of each sample foil were measured with a Ge(Li) detector, whose detection efficiency had been calibrated with a standard source of the mixed radioactive nuclei purchased

from Amersham. Nuclear data of half lives and gamma-ray intensities for the induced activities have been taken from the literature/9/.

#### NEUTRON ENERGY AND SPECTRUM FROM THE ${}^6\text{LiD}$ CONVERTERS

##### Neutron Energy

For the neutron energy determination around 14 MeV, two kinds of activation cross section curves are often used; one is almost constant and the other is linear dependent on neutron energy. The  ${}^{90}\text{Zr}(n,2n)$  and  ${}^{93}\text{Nb}(n,2n)$  reactions are usually selected for this purpose. The calibration curve of the reaction rate ratio versus neutron energy has been investigated by the several researchers, and Iguchi et al. summarized the results recently/4/. They have also proposed a semi-empirical formula for the curve of the Zr(n,2n)/Nb(n,2n) reaction rate ratio.

The Zr/Nb ratio obtained from the present measurement was  $1.35 \pm 0.04$ , which corresponded to  $14.05 \pm 0.07$  MeV using the semi-empirical formula which Iguchi et al. proposed/4/. These results are summarized in Fig. 2. The present value of neutron energy is in good agreement with that of 14.1 MeV in the literature/3/ within an experimental error and agrees well with other recent measurements by the activation ratio method. The uncertainty presently obtained is mainly due to statistical error and detection efficiency in their induced activity measurement.

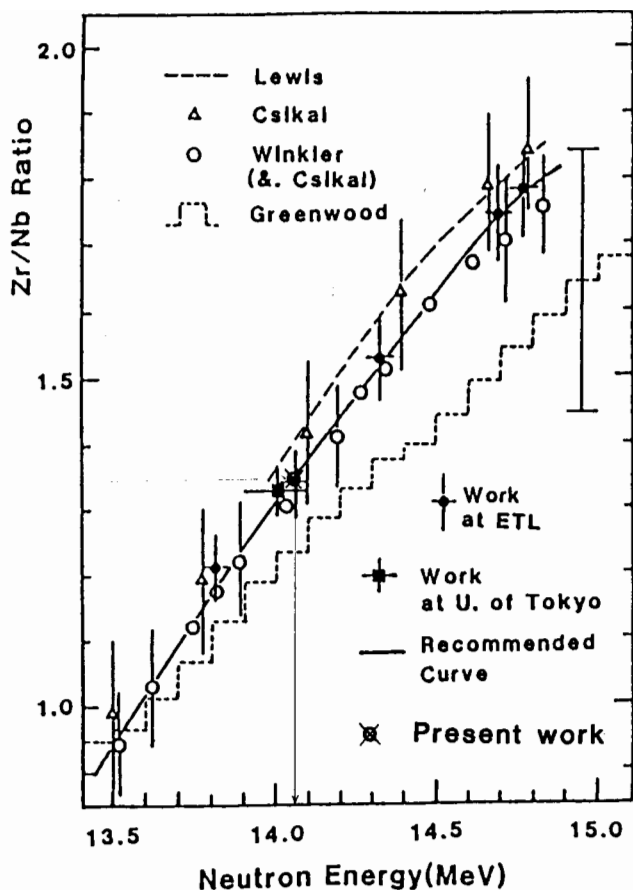


Fig. 2 Neutron energy dependencies of Zr/Nb activation rate ratio data.

#### Neutron Spectrum

In parallel with the spectrum measurement of the  ${}^6\text{LiD}$  converters, we have executed transport calculations by the ANISN code/7/. To apply a one dimensional geometry to the calculation, the converters were assumed to be a spherical shape with the same volume as the aluminum case, and set at the center of the mean radius to each wall of the irradiation room. Group constants of 137 were produced from the ENDF/B-IV data library with a processing code MAIL/10/. The number of quadrature points and the anisotropy of elastic scattering were taken to be 16( $S_{16}$ ) and 8( $P_8$ ), respectively.

In order to experimentally obtain the energy spectrum of neutrons from the  ${}^6\text{LiD}$  converters, we have employed the NEUPAC code, which was developed by Nakazawa et al./5,6/. The code contains energy dependent group cross section data and their error matrices for main important neutron dosimetry reactions in ENDF/B-V. The number of energy group is 135 in the region from 0.01 eV to 16.4 MeV, and 62 from 1 to 16.4 MeV.

From the thirteen kinds of dosimetry reaction rate data, variance and covariance data were produced as input data for the NEUPAC calculation. The initial guess spectrum for the NEUPAC calculation was taken from the transport calculation obtained above. The calculated spectrum shows a good agreement with that obtained by unfolding the thirteen kinds of activation data. The results

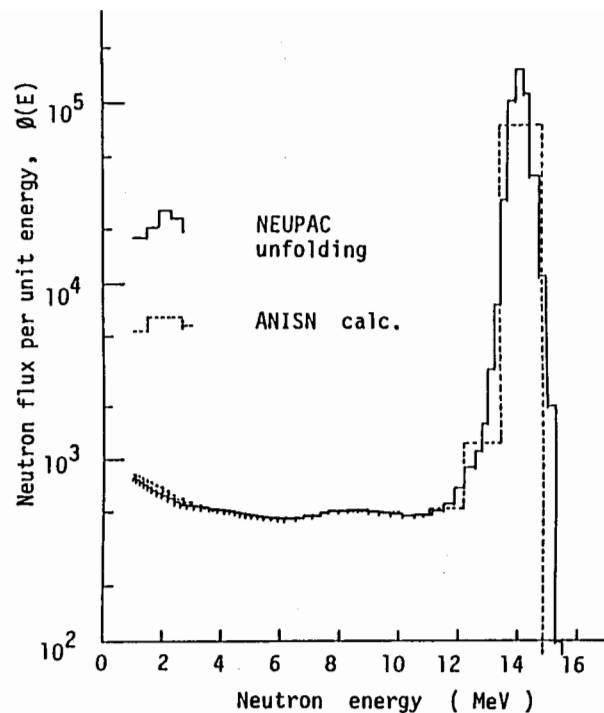


Fig. 3 Unfolded neutron spectrum from the  ${}^6\text{LiD}$  converters.

are shown in Fig. 3, where a peak can be seen at 14.1 MeV and small amount of slow neutrons below the peak can be observed. The full width at half maximum (FWHM) is about 1.6 MeV.

#### ACTIVATION CROSS SECTIONS MEASURED WITH THE ${}^6\text{LiD}$ CONVERTERS

As mentioned above, since we have measured the characteristics of the neutron energy and spectrum from the  ${}^6\text{LiD}$  converters, as seen in Figs. 2 and 3, we have applied the converter neutrons to the measurement of activation cross sections. The measured reaction rate per unit flux is related to the cross section as follows:

$$R_x = \frac{N_x \epsilon_x \int_{14 \text{ MeV}} \sigma(E) \phi(E) dE}{\int_{14 \text{ MeV}} \phi(E) dE}$$

where,  $N_x$ ,  $\epsilon_x$ ,  $\sigma(E)$  and  $\phi(E)$  are atomic density of the sample, detection efficiency, energy dependent cross section and the neutron energy spectrum from the converters, respectively.

The cross section for the  ${}^{27}\text{Al}(n, \alpha){}^{24}\text{Na}$  reaction in the ENDF/B-V dosimetry file has been selected as a standard value. For this reaction cross section, many data have been measured and evaluated. Moreover, the cross section curve shows a gentle slope depending on neutron energy near 14 MeV. The reference value obtained is  $123.0 \pm 3.8$  mb over the 14.1 MeV spectrum. The unknown cross section has been obtained relative to the reference cross section by using the following relation:

$$\sigma_x = \sigma_{Al} \frac{\epsilon_{Al} N_{Al} R_x}{\epsilon_x N_x R_{Al}}$$

where  $\sigma_{Al}$  is a standard value,  $\epsilon$ ,  $N$  and  $R$  are detection efficiency, atomic density of the sample and reaction rate which has been corrected for the effects due to slow neutrons below 12 MeV and for some other factors in the measurement, and the subscripts Al and x mean the data for aluminum and sample, respectively. The present results are summarized in Table 1, comparing with the evaluated cross sections taken from JENDL-2/11/, ENDF/B-V/12/ and the recent data/13,14/. We have given the correlation matrix in Table 2, whose data were produced from the variance-covariance data considering correlations between the measured data. The evaluated data and the recent data show a good agreement with the present measurements, especially except for the reactions of  $^{54}\text{Fe}(n,p)$  and  $^{93}\text{Nb}(n,2n)$ . For the former reaction, the experimental value is larger than the evaluations or other measurements. The difference is larger than the effects from the  $^{55}\text{Mn}(n,2n)$  reaction due to the manganese impurity of about 0.25 % in iron samples. This problem

has to be investigated. For the  $^{93}\text{Nb}(n,2n)$  reaction in JENDL-2, data from the ground and meta-stable states may be included in the evaluation.

#### REFERENCES

1. D. J. Hughes: "Pile Neutron Research", p.117, Addison-Wesley (1953).
2. M. A. Lone, et al.: Nucl. Instr. Meth., 174, 521 (1980).
3. W. H. Miller, et al.: Nucl. Instr. Meth., 216, 219 (1983).
4. T. Iguchi, et al.: J. Nucl. Sci. Technol., 24, 1076 (1987).
5. M. Nakazawa and A. Sekiguchi: Proc. 2nd ASTM-Euratom Symp. on "Reactor Dosimetry", NEREG/CP-00-4, Vol.3, 1423 (1977).
6. T. Taniguchi, et al.: NEUT Res. Rep. 83-10 (1983).
7. W. W. Engle, Jr.: K-1693 (1967).
8. T. Kobayashi, et al.: Annu. Rep. Res. Reactor Inst., Kyoto Univ., 18, 133 (1985).
9. C. M. Lederer and V. S. Shirley: "Table of Isotopes", 7th ed. John Wiley & Sons, Inc., New York (1978).
10. Y. Naito, et al.: JAERI-M 9396 (1981).

Table 1 Comparison of the present measurements and the recent data (in mb).

Reaction	Present	ENDF/B-V <sup>12)</sup>	JENDL-2 <sup>11)</sup>	IAEA Book <sup>13)</sup>	Ikeda <sup>14)</sup> *
$^{19}\text{F}(n,2n)^{18}\text{F}$	41.59 ± 1.70	- - -	42.94	55 ± 4	37.8 ± 2.0
$^{24}\text{Mg}(n,p)^{24}\text{Na}$	192.2 ± 6.6	- - -	- - -	181 ± 8	197.0 ± 9.8
$^{27}\text{Al}(n,\alpha)^{24}\text{Na}$	123.0 ± 3.8	123.0	120.9	119 - 121	123.6 ± 3.7
$^{27}\text{Al}(n,p)^{27}\text{Mg}$	77.07 ± 2.71	76.81	77.50	75 ± 4	70.6 ± 2.9
$^{46}\text{Ti}(n,p)^{46}\text{Sc}$	267.8 ± 9.3	257.7	- - -	242 ± 30	249 ± 13
$^{46}\text{Ti}(n,p)^{47}\text{Sc}$	289.6 ± 9.8	- - -	- - -	- - -	- - -
$^{48}\text{Ti}(n,p)^{48}\text{Sc}$	58.60 ± 1.88	63.50	- - -	66 ± 6	58.3 ± 2.8
$^{51}\text{V}(n,\alpha)^{48}\text{Sc}$	15.03 ± 0.65	- - -	15.00	16 ± 1.5	15.58 ± 0.81
$^{55}\text{Mn}(n,2n)^{54}\text{Mn}$	775.4 ± 28.6	722.3	770.9	809 - 890	752 ± 42
$^{54}\text{Fe}(n,p)^{54}\text{Mn}$	405.1 ± 15.3	359.6	359.9	332 - 365	343 ± 16
$^{56}\text{Fe}(n,p)^{56}\text{Mn}$	112.3 ± 3.9	108.8	113.9	98 ± 7	113.3 ± 5.8
$^{58}\text{Ni}(n,2n)^{57}\text{Ni}$	25.33 ± 0.83	25.35	21.50	30 ± 3	25.2 ± 1.3
$^{58}\text{Ni}(n,p)^{58}\text{Co}$	397.9 ± 13.3	415.3	400.0	375 - 378	356 ± 18
$^{59}\text{Co}(n,\alpha)^{56}\text{Mn}$	29.72 ± 1.04	28.95	30.00	29 ± 2	32.5 ± 1.6
$^{59}\text{Co}(n,2n)^{58}\text{Co}$	729.0 ± 29.0	749.0	639.9	720 - 788	705 ± 34
$^{64}\text{Zn}(n,p)^{64}\text{Cu}$	172.8 ± 12.7	- - -	- - -	160 - 164	- - -
$^{90}\text{Zr}(n,2n)^{89}\text{Zr}$	624.5 ± 20.5	- - -	- - -	764 - 768	613 ± 29
$^{90}\text{Zr}(n,2n)^{89m}\text{Zr}$	82.59 ± 5.01	- - -	- - -	86 ± 8	70.5 ± 4.1
$^{92}\text{Mo}(n,p)^{92m}\text{Nb}$	73.67 ± 4.14	- - -	61.40	60 - 64	72.6 ± 3.5
$^{93}\text{Nb}(n,2n)^{92m}\text{Nb}$	464.3 ± 15.1	- - -	1250	482 ± 35	469 ± 19
$^{115}\text{In}(n,n')^{115m}\text{In}$	65.03 ± 2.47	66.23	- - -	63 ± 6	- - -
$^{197}\text{Au}(n,2n)^{196}\text{Au}$	2125 ± 79	- - -	- - -	2160 ± 35	2004 ± 106
$^{204}\text{Pb}(n,2n)^{203}\text{Pb}$	1910 ± 63	- - -	2023	2103 ± 200	2155 ± 125
$^{204}\text{Pb}(n,n')^{204m}\text{Pb}$	63.81 ± 3.30	- - -	- - -	- - -	- - -

\* Calculation by the interpolation between the measured data

11. T. Nakagawa(ed.): JAERI-M 84-103 (1984).
12. ENDF/B-V dosimetry file (Tape=531), (1979).
13. IAEA, "Handbook on Nuclear Activation Data",  
Technical Reports Series No.273, IAEA (1987).
14. Y. Ikeda, et al.: JAERI 1312 (1988).

Table 2 Summary of the present results.

ROW/CI		OUTPUT	%	ABS ERR
1	AL27NA	1.230D+02	3.07	3.774D+00
2	AL27NP	7.707D+01	3.52	2.711D+00
3	NI58NP	3.979D+02	3.33	1.313D+01
4	NI8N2N	2.533D+01	3.27	8.286D-01
5	ZRON2N	6.245D+02	3.28	2.048D+01
6	NB3N2N	4.643D+02	3.25	1.508D+01
7	CO59NA	2.972D+01	3.50	1.040D+00
8	TI46NP	2.678D+02	3.47	9.293D+00
9	TINX7N	2.896D+02	3.37	9.760D+00
10	TI48NP	5.860D+01	3.21	1.883D+00
11	MN5N2N	7.754D+02	3.69	2.860D+01
12	ZRMN2N	8.259D+01	6.07	5.011D+00
13	F19N2N	4.159D+01	4.08	1.697D+00
14	FE54NP	4.051D+02	3.78	1.529D+01
15	FE56NP	1.123D+02	3.49	3.915D+00
16	CO9N2N	7.290D+02	3.98	2.901D+01
17	IN15NN	6.503D+01	3.80	2.471D+00
18	MG24NP	1.922D+02	3.46	6.641D+00
19	PB04NN	6.381D+01	5.17	3.299D+00
20	PB4N2N	1.910D+03	3.31	6.322D+01
21	V51NA	1.503D+01	4.31	6.470D-01
22	ZN64NP	1.728D+02	7.37	1.274D+01
23	MO92NP	7.367D+01	5.48	4.139D+00
24	AU7N2N	2.125D+03	3.70	7.863D+01

CORRELATION MATRIX ( PRINTED VALUE HAS BEEN MULTIPLIED BY 100. )

ROW/COL	1	2	3	4	5	6	7	8	9	10	11	12	13	14	15	16	17	18	19	20	21	22	23	24	
1	100																								
2	87	100																							
3	93	83	100																						
4	93	82	90	100																					
5	94	84	92	91	100																				
6	96	85	93	91	93	100																			
7	87	80	82	81	84	84	100																		
8	87	77	82	82	84	85	79	100																	
9	90	80	85	84	86	88	82	85	100																
10	92	82	87	86	89	90	83	86	85	100															
11	84	75	79	78	80	81	76	77	79	81	100														
12	51	46	48	48	49	50	47	46	49	48	44	100													
13	75	70	70	70	72	72	70	66	69	70	65	39	100												
14	80	73	75	75	76	77	73	71	73	75	73	41	65	100											
15	86	79	81	80	82	83	80	76	79	81	77	45	72	78	100										
16	77	71	72	71	73	74	72	68	70	72	66	40	66	66	74	100									
17	81	75	76	75	77	78	76	72	74	76	70	42	73	71	78	71	100								
18	90	79	85	84	86	88	79	82	83	87	77	47	68	73	78	69	73	100							
19	60	53	56	56	58	59	53	55	56	58	51	32	45	48	52	46	49	57	100						
20	90	79	84	84	86	87	80	83	90	84	77	48	68	73	78	69	73	85	56	100					
21	71	63	68	67	69	72	63	63	65	67	60	37	54	58	62	55	60	65	43	65	100				
22	41	36	38	38	39	39	37	36	37	38	37	21	32	38	39	33	34	37	25	37	29	100			
23	56	50	53	53	54	56	50	50	51	53	48	29	43	46	49	44	47	51	34	51	48	23	100		
24	83	74	79	78	80	84	74	74	76	78	72	43	64	69	74	65	71	76	51	75	70	33	57	100	